

弾性モードで振動する翼周りの非定常粘性流の数値シミュレーション

ケイランディシュ ハミドレザ、別府 護朗、中道 二郎

Numerical Simulation of Viscous Unsteady Flow Around Wing Oscillating in Elastic Modes

Hamidreza KHEIRANDISH¹⁾, Goro BEPPU²⁾ and Jiro NAKAMICHI³⁾

An aeroelastic version of CFD code was developed and applied to numerical simulations of unsteady transonic flows around a rectangular wing with bioconvex airfoil section oscillating in bending mode and a wind tunnel model of a high aspect-ratio (YXX) wing which is also oscillating in first bending mode. A numerical simulation of transonic flutter of the YXX wing considering first six modes has been performed as well. The code is based on Navier-Stokes (N-S) equations coupled with the structural equations. The N-S equations are integrated by Yee-Harten TVD scheme on dynamic grid, while the structural side is integrated by Wilson θ method.

Key Words Unsteady Flow, Oscillating Elastic Wing, Viscous Flow,

1. INTRODUCTION

The computation of aeroelastic characteristics in the transonic speed is of much current interest. Aeroelasticity is concerned with those phenomena which involve mutual interaction among inertial, elastic, and aerodynamic forces. Since high performance modern aircraft tends to possess a high level of flexibility in order to satisfy low weight and maneuverability requirement, the avoidance and prediction of aeroelastic problems such as flutter, buffet and, buzz are very important in aircraft design. To clarify these nonlinear problems, CFD tools based on Navier-Stokes(N-S) equations including turbulence model are needed. The remarkable progress in computing resources in the last decade, tied with advances in computational methods, has motivated the development of aeroelastic CFD codes. Prediction of flutter boundaries of a 3-dimensional elastic wing based on N-S equations is the final goal of this research.

In the present study, the time averaged N-S equations coupled with Baldwin-Lomax¹⁾ (B-L) turbulence model, were integrated by Yee-Harten²⁾ implicit TVD scheme. An ADI form which is of second order accuracy both in space and in time has been used.

To describe the effects of elastic oscillation of a wing on the flow stream and aerodynamic forces, the following two numerical simulations have been performed in advance:

a) numerical flow simulation around a rectangular wing oscillating in first bending mode with reduced frequency of .13 (based on the root half-chord and free stream velocity). The numerical results are compared with the experimental results³⁾ of wind tunnel tests.

b) numerical solution of the YXX wing oscillating in the first bending mode with reduced frequency of .381.

Finally numerical simulation of flutter of YXX wing in transonic region is presented. The flutter boundary is investigated and compared with experimental ones.

2. NUMERICAL IMPLEMENTATION

To calculate aeroelastic response of an elastic wing, it is needed to integrate the governing equations for the flow field and structural dynamic equations simultaneously. In the

present study, the governing equations are the unsteady N-S equations coupled with B-L turbulence model. The structural equations are derived by employing modal approach. Introducing generalized coordinates, so called flutter equations can be written in a nondimensional form as;

$$m_i \ddot{q}_i + k_i^2 m_i q_i = Q \iint_{\Delta} C_p \Phi_i n_z dS \quad (2.1)$$

where q_i are generalized coordinates, Φ_i and m_i are fundamental modes and generalized masses with respect to the i 'th mode, and where k_i and Q are the reduced frequencies and nondimensionalized dynamic pressure, respectively. The nonlinear aerodynamic loads of right hand side obtained by integrating N-S equations are substituted. The left hand side of Eqs.(2.1) is integrated by Wilson θ method⁴⁾.

The computation is proceeded in a time dependent manner with a specified dynamic pressure and the time histories of generalized coordinates are obtained. At a dynamic pressure, every q_i converges with respect to time. At another condition, it diverges statically or dynamically. In the former case, the static aeroelastic deformation of the wing can be obtained. In the latter cases, the system is unstable and divergence velocity or flutter dynamic pressure can be captured by looking at the time histories of the generalized coordinates.

In the present calculations, the following procedures are considered to update grid points at each time step. Having computed generalized coordinates, wing surface grid points are renewed by superposing the fundamental modes. To update the flow field grid points as fast as possible, moving grid strategy⁵⁾ is used at each time step. The deformation of wing, however, becomes too large after some amount of iterations and the above mentioned strategy no longer works well. Overlapping or skewness of grid lines occurs. So a grid generator, alternatively, was employed to renew the whole grid, in accordance with the new position of the wing surface, at every reasonable number of steps.

3. RESULTS AND DISCUSSIONS

Firstly, numerical solution of a rectangular wing oscillating in the first symmetric bending mode is presented. The wing is of aspect ratio 3 with bioconvex airfoil section (5% thickness-chord ratio). The mean angle of attack is 0 degree

1) Graduate Stud., Dept. of Aeronautics and Astronautics, Tokai Univ.

2) Prof., Dept. of Aeronautics and Astronautics Tokai Univ.

3) Head, Structural Mechanics Div., NAL

and Mach number is 0.9. The frequency is interpreted in terms of reduced frequency of 0.13. Reynolds number was settled to be 5×10^6 . The nondimensional wing tip amplitude is 0.011 based on the root chord length. The first bending mode shape is obtained from reference(3). The comparisons of unsteady pressure (upper/lower) difference distributions between the numerical results and experimental ones are given at four span positions in Fig. 1, which are shown in terms of magnitudes and phase angles. The results are relatively in good agreements with each other. The discrepancies between computed and experimental results at the wing root is due to boundary layer of the side wall of tunnel which wing is installed. Since the wall effect is not taken into account in this study, a shock also appears at wing root position, whereas in the experiment it does not.

In the second example, numerical solution of YXX wing oscillating in first bending mode is presented. The planform of this wing is given in Fig. 2. The aspect ratio of the wing is 10.0, the taper ratio is 0.324 and the quarter chord sweep angle is 18° . It has supercritical wing section, and a built-in nose down twist of 3.5° at the wing-tip. The angle of attack and Mach number of this case are 0 degree and 0.7, respectively. Reynolds number is 10^6 . The reduced frequency is set to be 0.381 which corresponds to frequency of 168 Hz (experimental flutter frequency). The steady state pressure distributions are given in Fig. 3. The amplitude of oscillation at the wing tip is about half root chord length. A C-H mesh with $179 \times 60 \times 51$ grid points was used. Real and imaginary parts of unsteady pressure distributions at four span positions, which are normalized by magnitude of oscillatory angle of attack at wing tip, are given in Fig. 4. To get some idea of the effect of this oscillation, pressure distributions on upper and lower surfaces are shown in Fig. 6. for 26 time sequence steps in the third cycle. The closer to the wing tip, the more variation of pressure distributions can be observed in a cycle. This comes from the changes of effective angles of attack due to the motion of wing surface. The time histories of lift and drag coefficients are given in Fig. 5. for the first three cycles.

Finally flutter simulation of YXX wing in transonic region is presented. The fundamental frequencies which are calculated theoretically and experimentally⁶⁾ are given in table 1. The shapes of wing deformations are approximated by superposing the first six fundamental modes obtained by vibration analyses of the wing. Classically, the linear theory was used to obtain the flutter velocity and the problem was reduced to an eigenvalue one. In the modern CFD aeroelasticity, the phenomena are simulated using high level of nonlinear flow modeling on computers. The procedure of the present flutter simulation is as follows;

- 1) set a low dynamic pressure
- 2) integrate Eqs.(2-1) and obtain the converged solutions; that is, static aerodynamic deformation
- 3) increase dynamic pressure and integrate Eqs.(2-1) using the solution of step (2) as an initial conditions
- 4) investigate the time histories of the wing responses
- 5) repeat (3)-(4) and find the flutter point

The Mach number range is 0.7 to 0.85, The Reynolds number based on the root-chord length is 2.4×10^6 and the steady state angle of attack is 0.0° . In this study the dynamic pressure is swept at a fixed Mach number and the wing responses for many cycles obtained. The cases studied in the present numerical simulations are summarized in a plan of dynamic pressure vs Mach number in Fig. 7. The flutter frequencies are also shown in Fig. 8. For the Mach numbers 0.7, 0.75. and .85 the wing responses converged at dynamic pressures 150, 78, 120kPa, respectively. They entered to unstable area with increasing the dynamic pressures upto 190, 100, 128kPa, respectively. However, for Mach number 0.8, where the wing responses converged at dynamic pressures 110kPa, the wing responses never diverged with increasing dynamic pressure for a large range upto 195kPa. It was found that the wing penetrated to low-damping(L-D)

area. The generalized coordinates q_1 , q_2 , and q_3 at dynamic pressures 110, 140, 160 and 195 kPa, and Mach number 0.8, are shown in Fig. 9. In low damping area the amplitude of generalized coordinates decreased rapidly after a few cycles of oscillations, specially q_1 , but they never tended to converge. The flutter test has only been conducted at two points for angle of attack, 0° . There is no report of low damping area in experiment at this angle of attack. However it was found in the numerical simulations at Mach number 0.8. The frequencies of the current results are in good agreement with the experimental ones. It is also found that the frequencies of oscillation in low damping area were higher than that of flutter point.

4. CONCLUSION

The developed computer codes have been already used to simulate, unsteady flows about oscillating NACA0012 airfoil, flutter of the same airfoil and, unsteady flows about YXX wing. It has been also applied to mentioned problems in this report. The comparisons of numerical results with experimental ones show that these codes are valid and powerful to clarify unsteady aerodynamic phenomena.

All simulations presented here were done on NWT parallel computer at NAL.

REFERENCES

- 1) Baldwin, B.S. and Lomax, H., "Thin Layer Approximation and Algebraic Model for Separated Turbulent Flows," AIAA paper, 78-257 (1978)
- 2) Yee, H. and Harten, A., "Implicit TVD Schemes for Hyperbolic Conservation Law in Curvilinear Coordinates," AIAA paper, No.85-1513 also AIAA Journal Vol.25, No.2, (1987), pp.266-274
- 3) Lessing, H.C., "Experimental Determination of the Pressure Distribution on a Rectangular Wing Oscillating in the First bending Mode for Mach Number From 0.24 to 1.3", NASA TND-344.
- 4) Bate, K.-J. and Wilson, E.L. "Numerical Methodes in Finite Element Analysis," Prentice-Hall (1976)
- 5) Nakamichi, J., "Calculation of Unsteady Navier-Stokes Equations Around an Oscillating 3-D Wing Using Moving Grid System," AIAA paper, 87-1158-CP
- 6) Kwasaki Heavy Industry KR-14465 (written in Japanese)

Table 1. Fundamental Frequencies of Flutter Model

Mode	Frequency Hz	
	Nastran	Experiment
First Bending	60.6	61.9
Second Bending	200.6	206.1
First Torsion	429.4	413.2
Third Bending	448.2	453.7
Second Torsion	702.4	-----
Third Torsion	816.9	-----

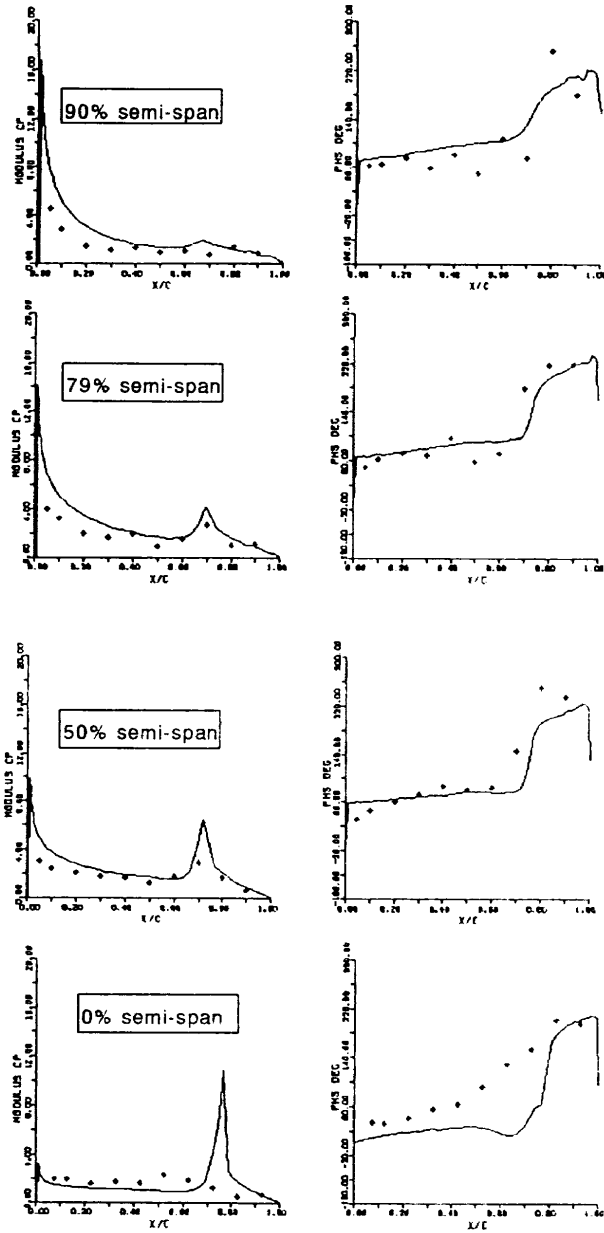


Fig. 1. Comparison of Magnitudes and Phase Angles Between Present Results and Experimental Ones (lines are present results)
 $\alpha=0.0$, $M=0.9$, $Re=5 \times 10^6$, $K=0.234$

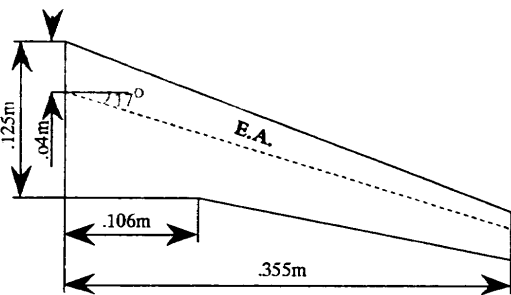


Fig. 2. Planform of YXX Wing Model

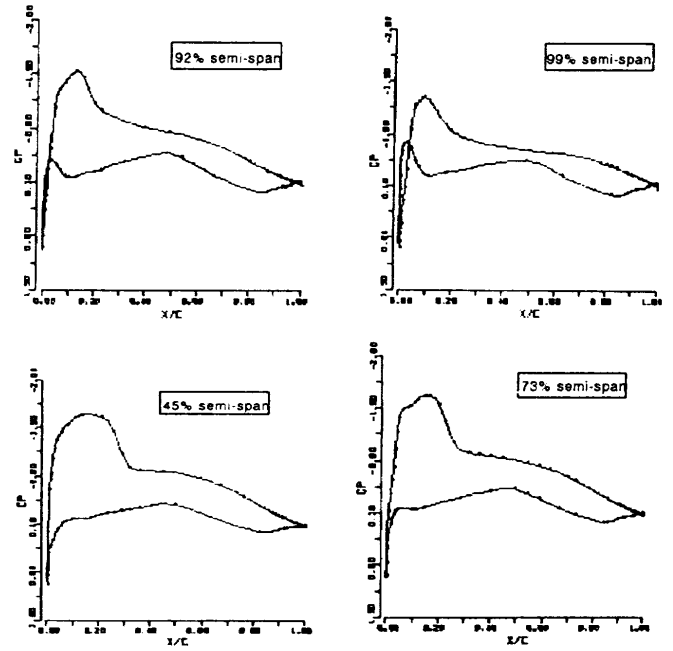


Fig. 3. Steady State Pressure Distributions
 $\alpha=0.0$, $M=0.7$, $Re=10^6$

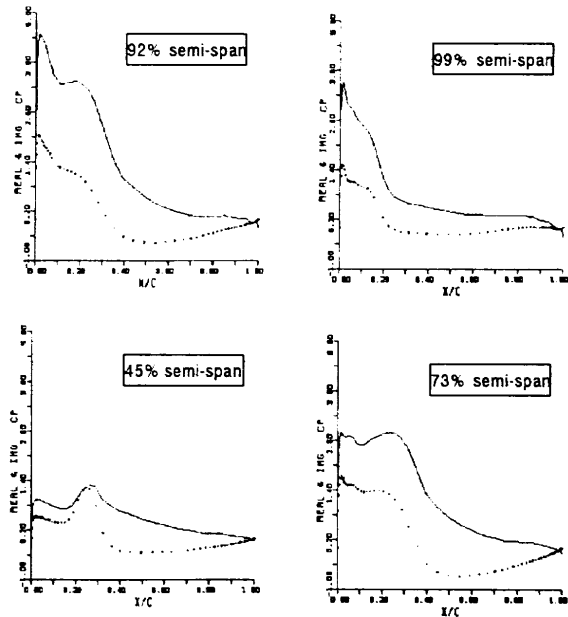


Fig. 4. Real and Imaginary Parts of Unsteady Pressure Distributions (lines are real part)
 $\alpha=0.0$, $M=0.7$, $Re=10^6$, $K=0.381$

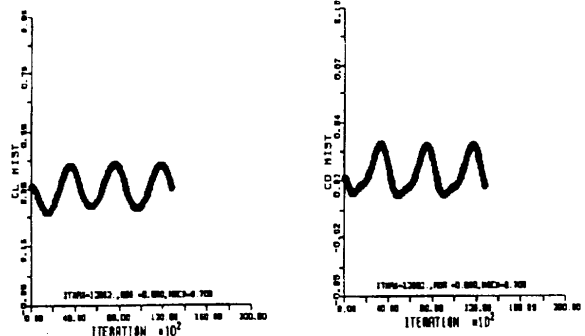


Fig. 5. Time Histories of Aerodynamic Forces

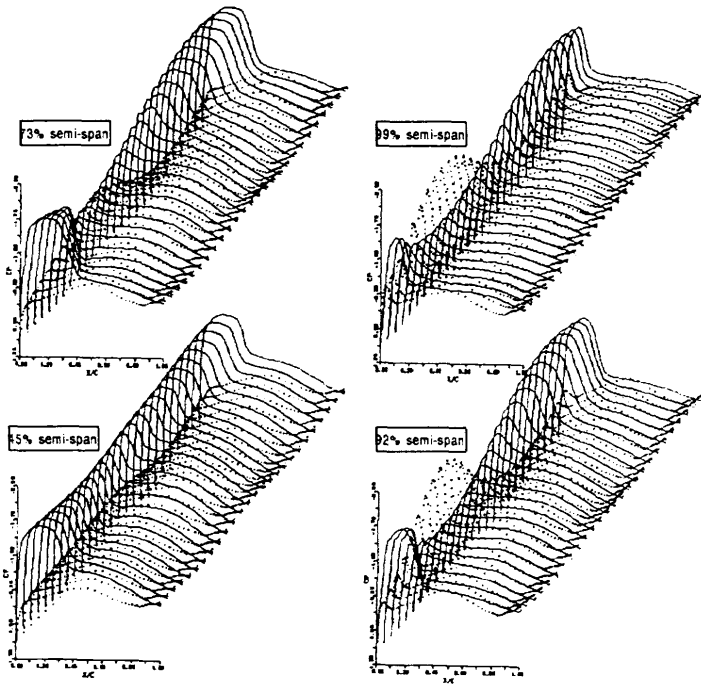


Fig. 6. Pressure Distributions of Upper and Lower Surfaces for One Cycle $\alpha=0.0$, $M=.7$, $R_e=10^6$, $K=.381$

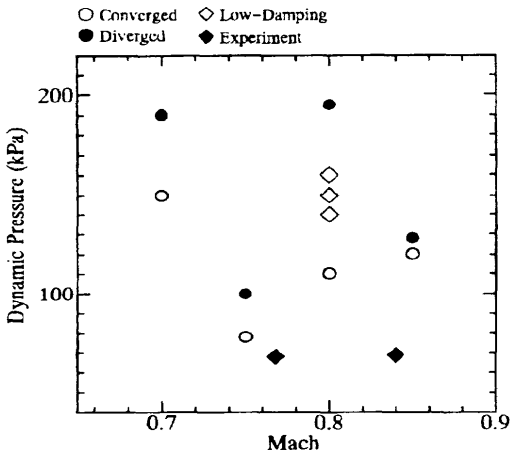


Fig 7. Flutter Boundary of YXX Wing Model ($\alpha=0.0^\circ$)

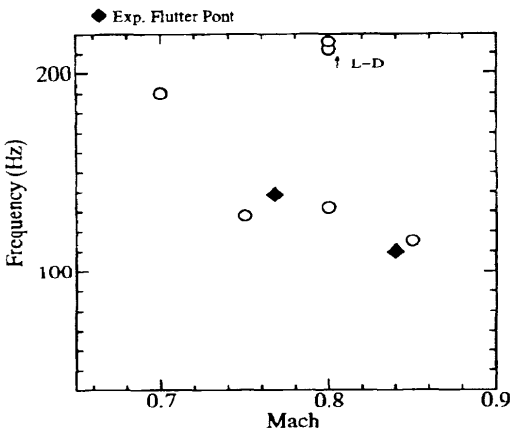


Fig 8. Frequency of Wing Response in Unstable Region ($\alpha=0.0^\circ$)

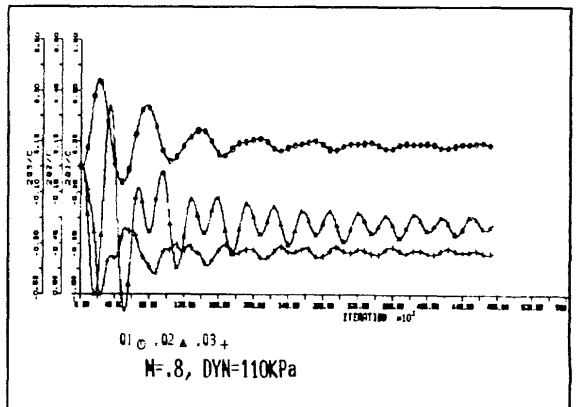
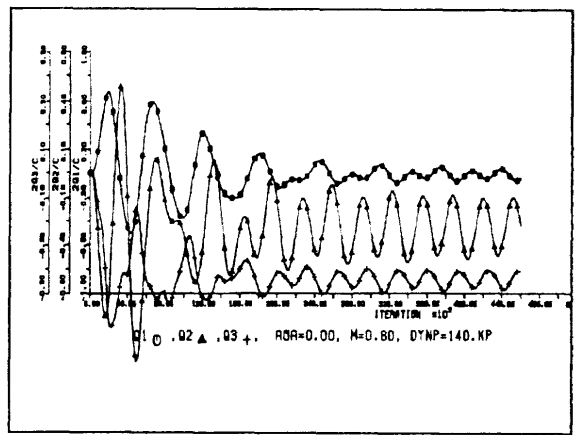
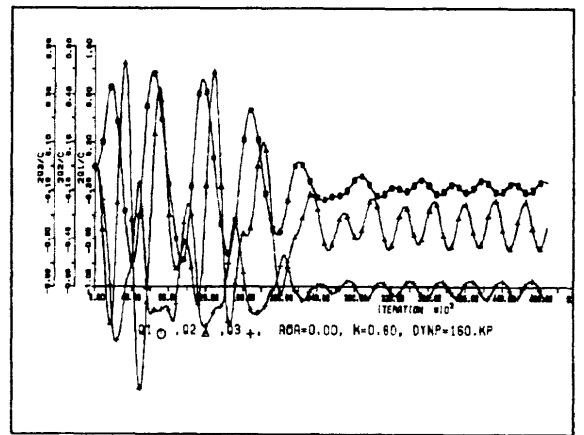
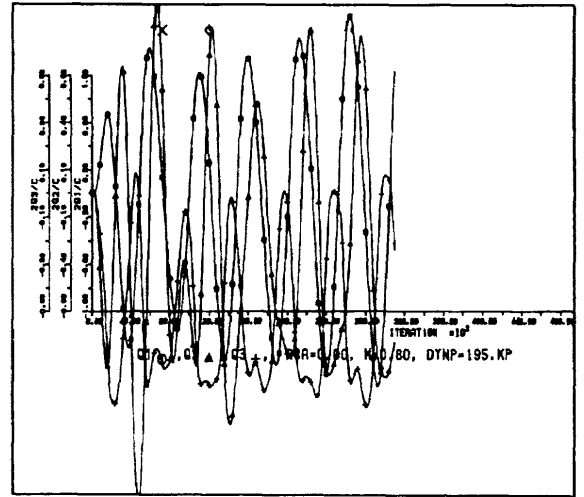


Fig. 9. Time Historeis of Wing Responses $\alpha=0.0$, $M=.8$, $R_e=2.4 \times 10^6$